pISSN 1598-298X
J Vet Clin 31(6) : 495-501 (2014)

Journal of Veterinary Clinics
www.ksvc.or.kr

Effect of Different CT Scanner Types and Beam Collimations on Measurements of Three-Dimensional Volume and Hounsfield Units of Artificial Calculus Phantom

Jihwan Wang and Heechun Lee[1]

Research Institute of Life Sciences, Gyeongsang National University, Jinju 660-701, Korea

(Accepted: December 08, 2014)

Abstract : The objective of this study was to evaluate the differences and reproducibility of Hounsfield unit (HU) value and volume measurements on different computed tomography (CT) scanner types and different collimations by using a gelatin phantom. The phantom consisting of five synthetic simulated calculus spanning diameters from 3.0 mm to 12.0 mm with 100 HU was scanned using a two-channel multi-detector row CT (MDCT) scanner, a four-channel MDCT scanner, and two 64-channel MDCT scanners. For all different scanner types, the thinnest possible collimation and the second thinnest collimation was used. The HU values and volumes of the synthetic simulated calculus were independently measured three times with minimum intervals of 2 weeks and by three experienced veterinary radiologists. ANOVA and Scheffé test for the multiple comparison were performed for statistical comparison of the HU values and volumes of the synthetic simulated calculus according to different CT scanner types and different collimations. The reproducibility of the HU value and volume measurements was determined by calculating Cohen's *k*. The reproducibility of HU value and volume measurements was very good. HU value varied between different CT scanner types, among different beam collimations. However, there was not statistically significant difference. The percent error (PE) decreased as the collimation thickness decreased, but the decrease was statistically insignificant. In addition, no statistically significant difference in the PEs of the different CT scanner types was found. It can be concluded that the CT scanner type insignificantly affects HU value and the volumetric measurement, but that a thinner collimation tends to be more useful for accurate volumetric measurement.

Key words **:** Computed tomography, Hounsfield unit, Volume measurement, Phantom.

Introduction

To form a computed tomography (CT) image, each pixel needs a Hounsfield unit (HU) value, which represents the density, and is proportional to the X-ray reduction rate in a voxel and represented as the linear attenuation coefficient (4). The HU value is proportional to the X-ray reduction rate in a voxel and is relatively set compared to air, water, and a compact bone when they are −1,000, 0, and +1,000, respectively (4). The HU value is used to quantify the images provided by CT.

The HU value can be used to differentiate a cyst from a tumor and to diagnose a soft tissue lesion by evaluating the presence or absence of a calcified substance or a fatty substance in the tumor (7,14,20). It can also be used to define diseases. For example, coronary artery calcification is defined as a disease that represents, overall, a more than 130 HU value in at least 2 mm^2 areas (3). The HU value is also used to diagnose osteoporosis and other metabolic bone diseases, and to evaluate the quality of the jawbone (12,16,27,28).

The HU value, however, is not totally dependent on the density of the object. It can also be affected by the beam hardening effect, scattered radiation, a difference between the image acquisition system and the reconstruction algorithms, the partial volume effect, the quantum mottle, and the object's location (10,18,22,24,25,39). Thus, the HU values of objects with the same density can differ. Thus, the range and cause of variations in HU values should be understood when HU values are used to diagnose a disease and to specify a tissue. These variations in the HU value is the unique problem of CT, and HU values can vary even with the recently developed CT scanner.

Volumetric measurement using CT can be performed for any structure included in the scan field, either by using automated measurement software or by hand-tracing the edges in sequential transverse images (8).

Although volumetric measurement of organs or lesions, including the liver (13), spleen (2), brain (15), hematoma (40), and pulmonary contusion (35), using CT has been reported in several literatures, the chief clinical applications of volumetric measurement are related to clinical oncology (9). In radiotherapy treatment planning, proper estimation of the tumor volume is essential to avoid tumor remission (30). In evaluating the response to chemotherapy, radiotherapy, or immunotherapy treatment, accurate volume definition may be a criterion in the assessment of the residual mass (30). In addition, to distinguish a benign-form malignant lung nodule, CT is used for close monitoring. The volume doubling rate is being given increasing attention as an indicator of malig-

[1]Corresponding author.
E-mail : lhc@gnu.ac.kr

nancy (19).

Recently, several studies in human medicine have attempted to assess whether urinary stone volumes and HU values using CT could be used to predict the stone fragility before extracorporeal shock wave lithotripsy (ESWL) (1,29). However, to the authors' knowledge, there are no reports in veterinary literature that document a study of predicting the therapeutic effect of ESWL using CT.

As the first step in the performance of various studies associated with predicting the therapeutic effect of ESWL using CT, the differences and reproducibility of HU value and volume measurements were tested for different CT scanner types and different collimations due to the routine use of a wide spectrum of scanner types and protocols.

Materials and Methods

Phantom construction (Fig 1)

A phantom was constructed with a 12 × 12 × 8.7 cm plastic container (Lock & Lock Co. Ltd., Seoul, Korea), gelatin (Daejung Chemicals & Metals Co. Ltd., Gyonggi-do, Korea), and five synthetic simulated calculus with 100 HU (Kyoto Kagaku Co. Ltd., Tokyo, Japan). The diameters of the spheres were 3, 5, 8, 10, and 12 mm. Their volumes were calculated using the volume formula for a sphere, as follows: volume = $(4/3)\pi r^3$. The calculated volumes were 14.13 mm^3, 65.42 mm^3, 267.95 mm^3, 523.33 mm^3, and 904.32 mm^3, respectively.

One hundred and forty-eight grams of unflavored gelatin was added to 1,000 mL double-distilled water. The mixture was gently stirred for 2-3 minutes to wet all the gelatin particles while avoiding clumping or introduction of excess air. Then the mixture was heated until the gelatin was dissolved completely. The gelatin mixture was poured into the container to a height of 3 cm while taking care not to minimize the air bubble formation, and was left to cool for approximately 30 minutes at 4°C. The five synthetic simulated calculus were lined up on the non-complete firm gelatin according to their diameters, in increasing order, and the container was filled with the non-warm and non-firm gelatin mixture. The phantom was placed at 4°C overnight until it was completely set.

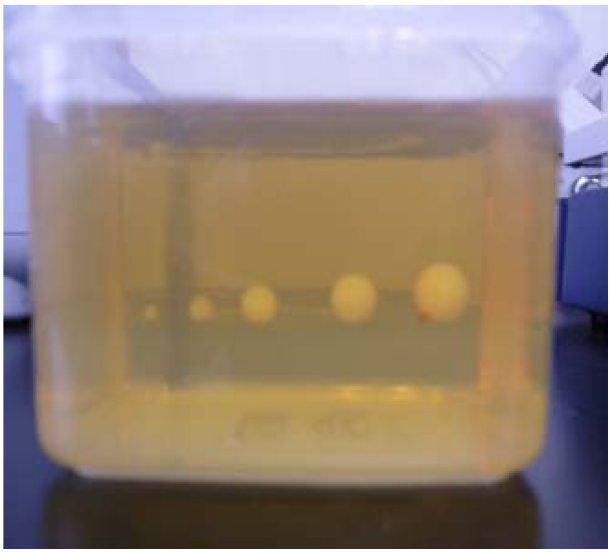

Fig 1. Artifical calculi phantom used for computed tomography.

CT protocols

Imaging was performed using a two-channel multi-detector row CT (MDCT) scanner (Somatom Emotion, Siemens Medical Systems, Erlangen, Germany), a four-channel MDCT scanner (LightSpeedQXi, General Electric Medical Systems, Milwaukee, WI, USA), and two 64-channel MDCT scanners (A: Brilliance 64, Philips Medical System, Best, The Netherlands and B: LightSpeed VCT, General Electric Medical Systems, Milwaukee, WI, USA). For each scanner, the calibration was checked immediately before the phantom data acquisition.

The image acquisition and reconstruction parameters for the individual CT scanners were as follows. For the Somatom Emotion, they were 120 kVp, 200 mAs, a 1.0 mm slice thickness, 1.0 and 1.5 mm detector collimations, a 1:1 pitch, a 10 cm field of view, and B40 reconstruction kernels. For the LightSpeedQXi, they were 120 kVp, 200 mAs, a 0.625 mm slice thickness, 0.625 and 1.25 mm detector collimations, a 1:1 pitch, a 10 cm field of view, and soft tissue reconstruction kernels. For the LightSpeed VCT, they were 120 kVp, 200 mAs, a 0.625 mm slice thickness, 0.625 and 1.25 mm detector collimations, a 1:1 pitch, a 10 cm field of view, and soft tissue reconstruction kernels. Finally, for the Brilliance 64, they were 120 kVp, 200 mAs, a 0.625 mm slice thickness, 64 × 0.625 and 16 × 0.625 mm detector collimations, a 1:1 pitch, a 10 cm field of view, and soft tissue reconstruction kernels. For all the different scanner types, the thinnest possible collimation and the second thinnest collimation were used, and all the images were reconstructed with the thinnest possible slice thickness.

HU value measurements of the synthetic simulated calculus

The HU value was measured with Lucion (Infinitt Technology, Seoul, Korea), which is a clinically used PC-based software. Among the cross-section images where synthetic simulated calculus were observed, the image with the largest synthetic simulated tumor was chosen, and the 3-4 mm^2 region of interest (ROI) was drawn. This measurement was performed in three sites, and the measured values were averaged. The synthetic simulated tumor with a 3 mm diameter was measured only once in one site.

Three-dimensional volumetric measurements of the synthetic stimulated calculus

Each dataset was transferred to a separate workstation. A special software (Lucion, Infinitt Technology, Seoul, Korea) was used for the three-dimensional (3D) volumetric measurement of the synthetic stimulated tumor. The initialization was performed with a rough diameter or a single click on the synthetic stimulated tumor either in the transverse, coronal, or sagittal view. Based on the click point, the algorithm estimated the volume of interest (VOI) around the lesion and the thresholds for the initial segmentation of the lesion via a histogram analysis within the VOI. Based on the calculated thresholds, the region-growing-based algorithm yielded the initial segmentation. Smaller adjacent structures with similar densities were excluded from the segmentation via morpho-

logical operations. An experienced radiologist performed the processing. To avoid bias, no manual editing of the segmentation results was allowed, though the software allows manual interaction and editing of the results.

To estimate the differences of the automated volume measurements, the percentage errors (PEs) were calculated using the formula $100 \times |V_{CT} - V_{true}|/V_{true}$, wherein V_{CT} and V_{true} are the automated measured and true known reference volumes, respectively. The calculated PE values were summarized according to means, corresponding standard deviations, and minimum and maximum.

Reproducibility of the HU value and 3D volume measurements

Three experienced veterinary radiologists participated in this study. Each examiner measured the HU value and volume of the synthetic simulated calculus. Each examiner was blinded to the measurement of the other examiners. One examiner (J.W) performed the measurement thrice with minimum intervals of 2 weeks to obtain an estimate for the intra-observer agreement.

Statistical analysis

All the data were statistically analyzed using one-way ANOVA and the multiple comparison Scheffé test at the significance level of 0.05. SPSS software (Version 14.0, SPSS, Inc., Chicago, Il, USA) was used in the analyses.

The reproducibility of the HU value and volume measurements was determined by calculating Cohen's *k*, which was interpreted according to the guidelines of Altman.

Results

Reproducibility of the HU value and 3D volume measurements

There was very good agreement among the HU value measurements of the synthetic simulated calculus by the three examiners with a *k* of 0.966. Very good intra-observer agreement with a *k* of 0.998 was also observed.

Similarly, inter-observer and intra-observer agreement of 3D volumetric measurements of synthetic simulated calculus were very good with a *k* of 0.999 and a *k* of 0.997, respectively.

Differences of the HU value measurements

The mean HU value for all the synthetic simulated calculus, including all the collimations and all the CT scan types, was 110.43 HU (± 6.182 HU, min 92 HU, and max 119 HU). Table 1 gives a summary of the observed HU values for the different CT scanner types and collimations.

The HU value data obtained when scanning the 100 HU synthetic simulated calculus demonstrated that the largest difference in the mean HU values for the 100 HU synthetic (113.46 ± 3.38 HU, min 108 HU, and max 118 HU) was that for the 64-channel MDCT scanner (GE) with a 1.25 mm collimation. Whereas the lowest difference in the mean HU value (104.86 ± 8.26 HU, min 92 HU, and max 112 HU) was that for the 64-channel MDCT scanner (Philips) with a 64 × 0.625 collimation. However, no statistically significant difference in the HU values in all the groups was found (Fig 2).

Table 1. Summary of HU values for different CT scanner types and different beam collimations

Scanner	Collimation (mm)	Average (HU)	SD (HU)	Min (HU)	Max (HU)
Siemens 2ch	1	111.74	6.87	101	119
	1.5	112.74	5.13	104	118
GE 4ch	0.625	112.28	4.69	104	116
	1.25	109.98	5.30	101	114
GE 64ch	0.625	112.28	2.98	108	116
	1.25	113.46	3.38	108	118
Philips 64ch	64 × 0.625	104.86	8.26	92	112
	16 × 0.625	106.09	8.31	93	114

HU: Hounsfield unit, CT: computed tomography, SD: standard deviation

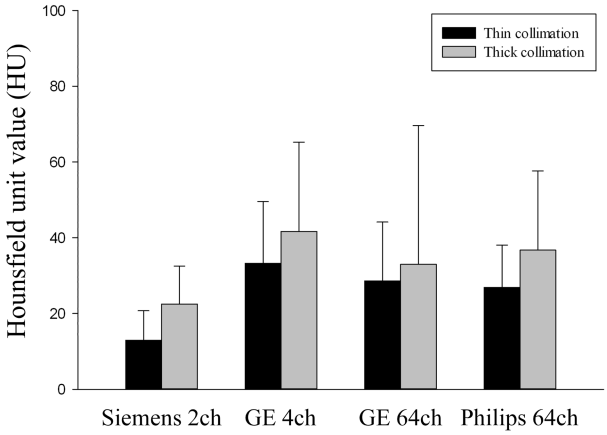

Fig 2. Hounsfield unit value variations according to different computed tomography scanner types and different beam collimations.

Table 2. Summary of PEs for different CT scanner types and different beam collimations

Scanner	Collimation (mm)	Average (%)	SD (%)	Min (%)	Max (%)
Siemens 2ch	1	12.94	7.79	7.63	26.35
	1.5	22.47	10.01	15.24	39.85
GE 4ch	0.625	33.23	16.30	18.97	59.96
	1.25	41.66	23.55	23.13	81.55
GE 64ch	0.625	28.56	15.57	16.29	55.57
	1.25	32.94	16.64	18.30	60.13
Philips 64ch	64 × 0.625	26.93	11.11	18.61	46.39
	16 × 0.625	36.70	20.96	22.14	73.61

PE: percent error, CT: computed tomography, SD: standard deviation

Differences of the 3D volume measurements

The mean PE for all the synthetic simulated calculus, including all the collimations and all the CT scan types, was

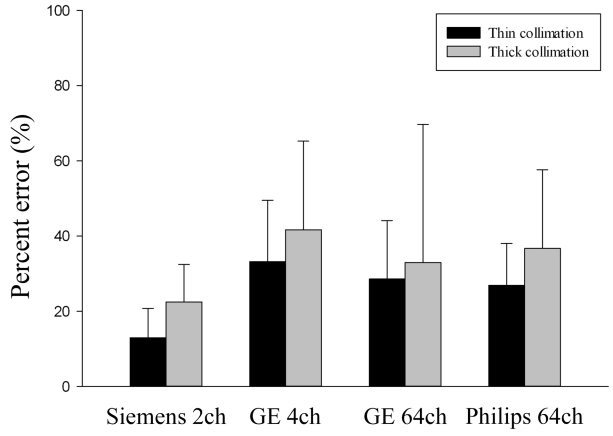

Fig 3. Percent error variations according to different computed tomography scanner types and different beam collimations.

29.43% (± 16.82%, min 24.05%, and max 34.81%). Table 2 gives a summary of the observed PEs for the different CT scanner types and collimations.

The lowest mean PE (12.93 ± 7.79%, min 3.26%, and max 22.61%) was that for the two-channel MDCT scanner (Siemens) with a 1 mm collimation. The PE was lower in the thinnest collimation than in the second thinnest collimation for the same scanner type, but the difference was statistically insignificant. Thus, no statistically significant difference in the PEs in all the groups was found (Fig 3).

Discussion

Though the objects had identical densities, the HU value could be obtained differently depending on the beam hardening effect, scattered radiation, the difference between the image acquisition system and the reconstruction algorithms, the partial volume effect, the quantum mottle, and the objects' location (10,18,22,24,25,29).

Scattered radiation can show a 3-10% error and usually occurs in the fourth-generation CT scanner that uses a fixed detector (26). The error caused by scattered radiation is negligible, however, because in reality, the collimator in each detector absorbs most of the scattered rays even when extensive scattered radiation occurs when a fan-shaped X-ray is used (26). In this study, the HU values due to collimation, when the same MDCT scanner type was used, did not significantly differ. This was deemed to have been because the scattered radiation occurred due to the difference between thin and thick collimation, and was not large enough to affect the HU value.

The HU value is expressed as the average density of substances in the pixel. Thus, it is determined by the higher-density substance when lower-density and higher-density substances co-exist in the pixel. This is called the partial volume effect, and this effect increases when the object is small or when a motion artifact is produced with the movement of the object (14). Thus, the HU value should be measured as far as possible from the borderline of two different tissues. In this study, the HU value was measured in each synthetic simulated tumor to minimize the partial volume effect that could occur in the borderline between the background of the adjacent phantom and the synthetic simulated tumor.

Groell *et al* (14) reported that the HU value can vary due to the image acquisition system and the reconstruction parameter; Groell *et al* (14), that the signal-to-noise ratio was differentiated by the slice thickness; and Taguchi *et al* (33), that the ROI that was used to determine the HU value sensitively affected the noise and that the size of the ROI was the key factor of the precision of the bone density measurements.

Inter-scanner variations in the HU value were observed in this study, but there were no statistically significant differences. This is considered due to the slice thickness, inter-machine variation, quantum mottle, and differences between the image acquisition system and the reconstruction algorithms. The thinnest slice possible was used for the MDCT. The thinnest slice used for the Siemens MDCT was 1 mm thick, however, whereas the thinnest slice for the MDCT of the other companies was 0.625 mm thick. Also, the image acquisition system and the reconstruction algorithms for the MDCT of each company varied. The ROIs that were used in this study were all circular and 3-4 mm^2 area, though. Though not all the samples had exactly the same size, the error deemed due to the ROI was negligible.

Phantom images were obtained in one shooting since the HU value can vary due to the location of the objects in the scanner. Variations due to the location were eliminated by setting the location of the ROI in the synthetic simulated tumor.

Previous studies have reported inter-scanner variations when measuring the HU (4,14,32). Birnbaum *et al* (4) reported that the HU values varied from −15 HU to 20 HU when a 0-HU insert was measured with the standard reconstruction algorithm, using different MDCT scanners. Groell *et al* (14) reported a statistically significant difference in the HU values with two CT scanners in each compartment except in air, and the HU values varied from 1 to 15 HU when 0-HU water was measured. In this study, a 100-HU synthetic simulated tumor was scanned with four different MDCTs under the same conditions, and the average HU values that were measured using each MDCT did not show a statistically significant difference. The HU value that was obtained with the Siemens two-channel MDCT was 112.74 HU, however, whereas that which was obtained with the Philips 64-channel MDCT was 104.86 HU, which showed an 8-HU difference.

Several studies have reported that the lung nodule volume was accurately measured via computer-aided volumetry, and computer-aided volumetry was particularly useful for measuring small nodules with a diameter of less than 1 cm (6,23). In addition, due to the high reproducibility of computer-aided volumetry, it has been reported to be a non-invasive method that can accurately assess lung nodule growth and the outcomes of pulmonary cancer treatment (5,19,37). In this study, the volume was also measured using computer-aided volumetry, which showed an overall high level of accuracy. In addition, the intra- and inter-observer agreements in this study were 0.997 and 0.999, respectively, which showed a high level of reproducibility, as in other studies (5,19,37).

Two-dimensional (2D) and 3D volumetric measurements are used for automated volumetric calculation. For the 2D volumetric measurement, the diameter is measured under the

assumption that an object is spherical in a transverse image, or the diameter of two directions is measured under the assumption that an object is oval After the area is calculated, the volume is calculated via extrapolation. In the 3D volumetric measurement that is based on the pixel attenuation, the volume of an irregularly shaped object is more accurately measured than in the 2D volumetric measurement, because the lung nodule data of the Z axis is included. Yankelevitzet *et al* (38) reported that a high level of accuracy with an error of 3% was achieved in a model study using 3D image extraction and that the 3D volumetric measurement was more accurate than the 2D volumetric measurement. In this study, though the results of the 3D volumetric measurement were not directly compared with those of the 2D volumetric measurement, the study was conducted using 3D volumetric measurement under the assumption that the 3D volumetric measurement would be more accurate than the 2D volumetric measurement.

A helical CT scan obtains the sequential data on an interest area by simultaneously moving patients with a gantry during the rotation of the X-ray tube (17). For 3D images taken with helical CT, various processes that include data acquisition, transverse image acquisition including reconstruction, and construction of 3D images using transverse images are required, among which the data acquisition process most significantly affects the final image quality, the 3D image, and the volume. Various CT imaging and reconstruction factors such as the window setting, slice thickness, field of view, tube current, and reconstruction kernels have been reported to affect the accuracy of volume measurement using helical CT (21,31,34,36). In fact, when a preliminary study was conducted to compare the PEs after the slice thickness was changed to 1 mm, 2 mm, and 3 mm, respectively, under the same imaging condition as that in this study in which a two-channel MDCT scanner was used, the PE was shown to have decreased as the slice thickness decreased. In particular, a statistically significant difference in the PE was found between the 1 mm and 3 mm slice thicknesses.

Yankelevitzet *et al* (38) reported that a volume error of 3% or less was shown when the synthetic nodule volume was measured using a thin collimation and a small field of view. In addition, Das *et al* (11) measured the synthetic nodule volume using thin and thick collimations and reported that the volume that was measured using a thin collimation was more accurate than that measured using a thick collimation in the PE comparison. As the CT resolution varies depending on the CT scanner type and the beam collimation, the results of the segmentation may vary. Thus, this study was conducted under the assumption that the accuracy of the volume measurement would be affected. When the volumes of the different CT scanner types were compared according to their collimations, the PE was lower in the thin than in the thick collimation, but the difference was statistically insignificant. In addition, when the PEs of all the groups were compared, no statistically significant difference was found.

The current study had some limitations. First, scan acquisition parameters for every scanner evaluated were not standardized owing to differences in MDCT design. Second, the synthetic simulated calculi used in this study were the spherical types with a flat boundary. Thus, no comparative study was conducted with an irregularly shaped object that is used in clinical practice. Finally, in this study, the inter-scanner variations between different HU values were not evaluated because only 100-HU synthetic simulated calculi were used. Thus, further comparative studies are required.

In conclusion, the differences of volume and HU value of the simulated synthetic tumor were estimated using various CT scanner types and collimations. HU value varied between different CT scanner types, among different beam collimations. However, there was not statistically significant difference. The PE decreased as the collimation thickness decreased, but the decrease was statistically insignificant. In addition, no statistically significant difference in the PEs of the different CT scanner types was found. Therefore, it can be concluded that the CT scanner type insignificantly affects HU value and the volumetric measurement, but that a thinner collimation tends to be more useful for accurate volumetric measurement.

Acknowlegment

This work was supported by the Gyeongsang National University Fund for Professors on Sabbatical Leave, 2013.

References

1. Bandi G, Meiners RJ, Pickhardt PJ, Nakada SY. Stone measurement by volumetric three-dimensional computed tomography for predicting the outcome after extracorporeal shock wave lithotripsy. BJU Int 2009; 103: 524-528.
2. Bezerra AS, D'lppolito G, Faintuch S, Szejnfeld J, Ahmed M. Determinations of splenomegaly by CT: is there a place for a single measurement? Am J Roentgenol 2005; 184: 1510-1513.
3. Bielak LF, Kaufmann RB, Moll PP, McCollough CH, Schwartz RS, Sheedy II PF. Small lesions in the heart identified at electron beam CT: calcification or noise? Radiology 1994; 192: 631-636.
4. Birnbaum BA, Hindman N, Lee J, Babb JS. Multi-detector row CT attenuation measurements: assessment of intra- and interscanner variability with an anthropomorphic body CT phantom. Radiology 2007; 242: 109-119.
5. Bolte H, Riedel C, Jahnke T, Inan N, Freitag S, Kohl G, Heller M, Biederer J. Reproducibility of computer-aided volumetry of artificial small pulmonary nodules in ex vivo porcine lungs. Invest Radiol 2006; 41: 28-35.
6. Bolte H, Riedel C, Müller-Hülsbeck S, Freitag-Wolf S, Kohl G, Drews T, Heller M, Biederer J. Precision of computer-aided volumetry of artificial small solid pulmonary nodules in ex vivo porcine lungs. Br J Radiol 2007; 80: 414-421.
7. Bosniak MA. The current radiological approach to renal cysts. Radiology 1986; 158: 1-10.
8. Breiman RS, Beck JW, Korobkin M, Glenny R, Akwari OE, Heaston DK, Moore AV, Ram PC. Volume determinations using computed tomography. Am J Roentgenol 1982; 138: 329-333.
9. Buthiau D, Antoine EC, Nizri D, Stefani E, Lucien P, Cohen-Aloro G, Gozy M, Guinet F, Chiche B, Weil M, Khayat D. The clinical measurement of volumes using helical CT. Surg Radiol Anat 1996; 18: 227 - 231.
10. Cann CE. Low-dose scanning for quantitative spinal mineral analysis. Radiology 1981; 140: 813-815.

11. Das M, Mühlenbruch G, Katoh M, Bakai A, Salganicoff M, Stanzel S, Mahnken AH, Günther RW, Wildberger JE. Automated volumetry of solid pulmonary nodules in a phantom: accuracy across different CT scanner technologies. Invest Radiol 2007; 42: 297-302.
12. Duckmanton NA, Austin BW, Lechner SK, Klineberg IJ. Imaging for predictable maxillary implants. Int J Prosthodont 1994; 7: 77-80.
13. Fritschy P, Robotti G, Schneekloth G, Vock P. Measurement of liver volume by ultrasound and computed tomography. J Clin Ultrasound 1983; 11: 299-303.
14. Groell R, Rienmuller R, Schaffler GJ, Portugaller HR, Grainf E, Willfurth P. CT number variations due to different image acquisition and reconstruction parameters: a thorax phantom study. Comput Med Imaging Graph 2000; 24: 53-58.
15. Hamano K, Iwasaki N, Kawashima K, Takita H. Volumetric quantification of brain volume in children using sequential CT scans. Neuroradiology 1990; 32: 300-303.
16. Kalender WA, Felsenberg D, Louis O, Lopez P, Klotz E, Osteaux M, Fraga J. Reference values for trabecular and cortical vertebral bone density in single and dual- energy quantitative computed tomography. Eur J Radiol 1989; 9: 75-80.
17. Kalender WA, Seissler W, Klotz E, Vock P. Spiral volumetric CT with single-breath-hold technique, continuous transport, and continuous scanner rotation. Radiology 1990; 176: 181-183.
18. Kemerink GJ, Lamers RJ, Thelissen GR, van Engelshoven JM. Scanner conformity in CT densitometry of the lungs. Radiology 1995; 197: 749-752.
19. Ko JP, Marcus R, Bomsztyk E, Babb JS, Stefanescu C, Kaur M, Naidich DP, Rusinek H. Effect of blood vessels on measurement of nodule volume in a chest phantom. Radiology 2006; 239: 79-85.
20. Korobkin M, Brodeur FJ, Yutzy GG, Francis IR, Quint LE, Dunnick NR, Kazerooni EA. Differentiation of adrenal adenomas from nonadenomas using CT attenuation values. Am J Roentgenol 1996; 166: 531-536.
21. Larici AR, Storto ML, Torge M, Mereu M, Molinari F, Maggi F, Bonomo L. Automated volumetry of pulmonary nodules on multidetector CT: influence of slice thickness, reconstruction algorithm and tube current. Preliminary results. Radiol Med 2008; 113: 29-42.
22. Levi C, Gray JE, McCullough EC, Hattery RR. The unreliability of CT numbers as absolute values. Am J Roentgenol 1982; 139: 443-447.
23. Marten K, Engelke C. Computer-aided detection and automated CT volumetry of pulmonary nodules. Eur Radiol 2007; 17: 888-901.
24. McCollough CH, Kaufmann RB, Cameron BM, Katz DJ, Sheedy II PF, Peyser PA. Electron-beam CT: use of a calibration phantom to reduce variability in calcium quantitation. Radiology 1995; 196: 159-165.
25. McCullough EC, Morin RL. CT-number variability in thoracic geometry. Am J Roentgenol 1983; 141: 135-140.
26. Merritt RB, Chenery SG. Quantitative CT measurements: the effect of scatter acceptance and filter characteristics on the EMI 7070. Phys Med Biol 1986; 31: 55-63.
27. Ohara T, Hirai T, Muro S, Haruna A, Terada K, Kinose D, Marumo S, Ogawa E, Hoshino Y, Niimi A, Chin K, Mishima M. Relationship between pulmonary emphysema and osteoporosis assessed by CT in patients with COPD. Chest 2008; 134: 1244-1249.
28. Papadakis AE, Karantanas AH, Papadokostakis G, Damilakis J. Assessment of the morpho-densitometric parameters of the lumbar pedicles in osteoporotic and control women undergoing routine abdominal MDCT examinations. J Bone Miner Metab 2011; 29: 352-358.
29. Pareek G, Armenakas NA, Fracchia JA. Hounsfield units on computerized tomography predict stone-free rates after extracorporeal shock wave lithotripsy. J Urol 2003; 169: 1679-1681.
30. Prabhakar R, Ganesh T, Rath GK, Julka PK, Sridhar PS, Joshi RC, Thulkar S. Impact of different CT slice thickness on clinical target volume for 3D conformal radiation therapy. Med Dosim 2009; 34: 36-41.
31. Ravenel JG, Leue WM, Nietert PJ, Miller JV, Taylor KK, Silvestri GA. Pulmonary nodule volume: effects of reconstruction parameters on automated measurements - a phantom study. Radiology 2008; 247: 400-408.
32. Sande EP, Martinsen AC, Hole EO, Olerud HM. Interphantom and interscanner variations for Hounsfield units-establishment of reference values for HU in a commercial QA phantom. Phys Med Biol 2010; 55: 5123-5135.
33. Taguchi A, Tanimoto K, Ogawa M, Sunayashiki T, Wada T. Effect of size of region of interest on precision of bone mineral measurements of the mandible by quantitative computed tomography. Dentomaxillofac Radiol 1991; 20: 25-29.
34. Van Hoe L, Haven F, Bellon E, Baert AL, Bosmans H, Feron M, Suetens P, Marchal G. Factors influencing the accuracy of volume measurements in spiral CT: a phantom study. J Comput Assist Tomogr 1997; 21: 332-338.
35. Wang S, Ruan Z, Zhang J, Jin W. The value of pulmonary contusion volume measurement with three-dimensional computed tomography in predicting acute respiratory distress syndrome development. Ann Thorac Surg 2011; 92: 1977-1983.
36. Way TW, Chan HP, Goodsitt MM, Sahiner B, Hadjiiski LM, Zhou C, Chughtai A. Effect of CT scanning parameters on volumetric measurements of pulmonary nodules by 3D active contour segmentation: a phantom study. Phys Med Biol 2008; 53: 1295-1312.
37. Wormanns D, Kohl G, Klotz E, Marheine A, Beyer F, Heindel W, Diederich S. Volumetric measurements of pulmonary nodules at multi-row detector CT: in vivo reproducibility. Eur Radiol 2004; 14: 86-92.
38. Yankelevitz DF, Reeves AP, Kostis WJ, Zhao B, Henschke CI. Small pulmonary nodules: volumetrically determined growth rates based on CT evaluation. Radiology 2000; 217: 251-256.
39. Zerhouni EA, Spivey JF, Morgan RH, Leo FP, Stitik FP, Siegelman SS. Factors influencing quantitative CT measurements of solitary pulmonary nodules. J Comput Assist Tomogr 1982; 6: 1075-1087.
40. Zimmerman RD, Maldjian JA, Brun NC, Horvath B, Skolnick BE. Radiologic estimation of hematoma volume in intracerebral hemorrhage trial by CT scan. Am J Neuroradiol 2006; 27: 666-670.

인공결석모형물의 부피와 하운스필드값 측정에 대한 전산화단층촬영기기의 타입과 빔 콜리메이션의 영향

왕지환 · 이희천[1]

경상대학교 생명과학연구원

요 약 : 본 연구는 다양한 전산화단층촬영기기와 촬영 프로토콜의 차이에 따른 모형물의 부피와 Hounsfield unit (HU) 수치의 차이를 평가하고 이 후 전산화단층촬영술을 이용하여 결석의 부피와 HU 수치를 포함한 다양한 인자들을 평가하고 이 중 체외충격파쇄석술에 의한 결석의 분쇄를 예측할 수 있는 인자를 찾고자 하였다. 다양한 직경의 100 HU 인공종양 5개를 (직경 3.0-12.0 mm) 이용하여 모형물을 만들었으며, 이 모형물의 부피와 HU 수치를 Siemens사의 2채널, GE사의 4채널과 64채널, 그리고 Philips사의 64채널 전산화단층촬영기기를 사용하여 평가하였다. 또한 각각의 전산화단층촬영기기에서 동일한 조건으로 collimation만 thin collimation과 thick collimation으로 변화를 주어 모형물을 촬영한 후 모형물의 부피와 HU 수치를 평가하였다. 평가자간 (inter-observer) 재현성을 평가하기 위해 3명의 수의영상의학 전공의가 연구에 참여하였으며 이중 한 명의 수의사가 평가자내 (intra-observer) 재현성을 평가하기 위해 모형물의 부피와 HU 수치를 2주 간격으로 총 3번 측정하였다. 부피의 평가자간 재현성과 평가자내 재현성은 $\kappa = 0.9994$, $\kappa = 0.9969$로 아주 우수하였으며, HU 수치의 평가자간 재현성과 평가자내 재현성 역시 $\kappa = 0.9984$, $\kappa = 0.9655$로 아주 우수하였다. 다양한 전산화단층촬영기기와 collimation 차이에 따른 부피와 HU 수치의 차이는 모두 통계학적으로 유의적인 차이를 나타내지 않았다. 그러나 부피의 경우 collimation이 얇을수록 부피의 정확도가 증가하는 경향을 보였다. 본 연구 결과를 토대로 향후 진행될 결석의 부피 및 HU 수치의 평가 시 전산화단층촬영기기의 차이에 따른 영향을 받지 않으리라 판단되어 Siemens사의 2채널 전산화단층촬영기기만을 사용하였으며, 비록 통계학적으로 유의적인 차이는 없었지만 부피의 정확도를 더 높이기 위하여 얇은 collimation을 사용하였다.

주요어 : 전산화단층촬영술, 하운스필드값, 부피측정, 모형물